Theory of a coherent atomic-beam generator

A. M. Guzmán,* M. Moore, and P. Meystre
Optical Sciences Center and Department of Physics, University of Arizona, Tucson, Arizona 85721
(Received 7 September 1995)

We present a many-body theory of a driven and damped trapped gas of interacting bosons, and demonstrate that one of the trap levels can become coherently populated, thereby leading to a coherent atomic-beam generator, or ''laser for atoms.'' The specific system we consider consists of a sample of bosonic atoms interacting via the near-resonant dipole-dipole interaction. The transverse center-of-mass motion of the atoms is confined by a two-dimensional potential well created by an array of cooling laser beams, while their longitudinal motion is quantized by a Fabry-Pérot for atoms. Under appropriate conditions, the dipole-dipole selection rules lead to the simplification that only two quantized levels of atomic motion need to be considered explicitly, the other levels being treated as reservoirs. One of the two levels is the ''pump level,'' while the other is the one where atomic coherence builds up (the ''lasing'' level). The master equation describing the dynamics of these levels can be solved numerically, and its solution exhibits a ''threshold behavior'' with a transition from super-Poissonian to Poissonian atom statistics in the ''lasing mode.''

PACS number(s): 42.50.Vk, 03.75.Fi, 32.80.Pj, 42.50.Ct

I. INTRODUCTION

The fact that it now appears possible to optically manipulate atoms systems in mesoscopic quantum states, both linearly and nonlinearly, opens up exciting new avenues of investigation, from fundamental studies of the transition between microscopic and macroscopic systems, to applied topics such as the design and realization of a coherent atomic beam generator, or ''laser for atoms.'' The goal of the present paper is to propose and analyze in some detail such a device.

Several groups are actively studying coherent atomic-beam generators. The schemes proposed so far can be loosely separated into two categories: the first one considers noninteracting atoms, or more precisely elastic collisions only, and relies on the so-called ''Bose enhancement factor'' to coherently populate a given mode of some atomic trap or resonator [1–3]. The neglect of inelastic atom-atom interactions in these proposals raises serious questions about their practicality. In contrast, the scheme that we propose relies explicitly on inelastic atom-atom interactions to achieve ''lasing.'' As such, it is quite similar to the general proposal by Holland *et al.* [4], although its specifics are substantially different.

It should be noted at the onset that there is a fundamental difference between Bose condensation [5,6] and a coherent atomic-beam generator, the first one being an equilibrium phenomenon while the second is predicted to occur in a driven system. Hence, the coherence properties of the ''atom laser'' are expected to be quite different from those of a Bose condensate.

The coherent atomic-beam generator (CAB) that we propose is based on a generalization of the nonlinear optical cavity recently analyzed in Ref. [7], and relies explicitly on the occurrence of long-range two-body collisions in its dynamics: The de Broglie waves resonator achieves the longitudinal confinement of matter waves via a Fabry-Pérot for atoms [8], the end mirrors being formed, e.g., by focused laser beams or by evanescent waves. In addition, transverse confinement is achieved by the quasiharmonic wells generated by laser cooling beams. As shown, e.g., in Ref. [9], even if the cooling laser beams are detuned sufficiently far from resonance to allow for the adiabatic elimination of the excited electronic states of the atoms, the ground-state trapped atoms are subjected to a two-body dipole-dipole interaction potential arising from their coupling to the vaccuum modes of the electromagnetic field [10,11]. Due to their long-range character these collisions present the significant advantage of producing the nonlinearity required to achieve stimulated amplification of the population of one of the cavity modes at reasonably low densities. In addition, their cross section can be tuned over several orders of magnitude by varying system parameters including the atom-field detuning and the precise geometry of the cavity. We will show how, in combination with cavity losses, these two-body interactions permit one to build a nearly Poissonian atomic distribution in one of the cavity modes.

Section II presents our model, discusses the geometry of the CAB cavity, and introduces the dipole-dipole interaction between atoms. This interaction is considered in more detail in Sec. III, where we show that it leads to selection rules that permit one to restrict the dynamics of the system to just a few cavity modes. Section IV discusses the CAB dynamics, using second quantization to describe the evolution of the occupation of the cavity modes of interest. The pump and loss mechanisms are described by a master equation, which is also introduced in that section. In Sec. V, we then turn to a numerical solution of this master equation, and show that ''laser'' action can be achieved for quasirealistic choices of parameters. Finally, Sec. VI is a summary and conclusion.

II. MODEL

We consider the matter waves resonator schematically represented in Fig. 1. The atomic mirrors are separated by a

* Permanent address: Departamento de Física, Universidad Nacional de Colombia, Bogotá, Colombia.

distance L along the $0z$ axis of atomic motion. The properties of a Fabry-Pérot for atoms operating in the quantum regime have been previously discussed [8]. We consider explicitly the case of large detunings between the atomic transition under consideration and the light fields, so that the excited atomic states can be adiabatically eliminated and we need consider the atomic ground states only. This is important if spontaneous heating, which is bound to be detrimental to CAB operation, is to be minimized. For the appropriate sign of the detuning, the light-induced atomic mirrors provide a repulsive potential for the center-of-mass motion of ground-state atoms and lead to a quasidiscrete set of resonant longitudinal modes for the atomic de Broglie waves. Their number and tunneling losses depend on the height and width of the potential barriers. In addition to this longitudinal trapping, transverse confinement of the atoms is produced by two counterpropagating lasers in a lin$\|$lin configuration [12], and is assumed to be uniform along $0z$.

The cooling laser beams are assumed to produce a series of quasiharmonic wells that transversally confine the atoms to better than a wavelength, which has been achieved experimentally [13–15]. For noninteracting atoms confined within one such well, the low-lying eigenstates of center-of-mass motion can be approximated by Hermite-Gaussian functions

$$\chi_{uv}(x,y)=\frac{1}{W_T\sqrt{2^{u+v}\pi u!v!}}\times\exp\left[-\frac{x^2+y^2}{2W_T^2}\right]H_u(x/W_T)H_v(y/W_T), \quad (1)$$

where u and v are integers equal to zero or positive, with corresponding eigenenergies

$$E_{uv}=(u+v+1/2)\hbar\Omega_T. \quad (2)$$

Here $\hbar\Omega_T=\sqrt{2U_0E_R}$, U_0 is the depth of the optical potential, and $E_R=\hbar^2k_L^2/2M$ is the atomic recoil energy for the cooling laser of wave number k_L. For simplicity, we neglect the effects of gravity, which acts along $0x$ and shifts the transverse equilibrium position of the atoms. We furthermore approximate the longitudinal eigenstates of the resonator by sinelike functions

$$\phi_\ell(z)=\sqrt{2/L}\sin(\kappa_\ell z), \quad (3)$$

where $\kappa_\ell=k_\ell-\imath\sigma_\ell$ are complex wave numbers with

$$k_\ell=\pi\ell/L, \quad (4)$$

ℓ being an integer. Their imaginary part accounts for losses, due, e.g., to tunneling through the positive constant σ_ℓ. For $\sigma_\ell\ll k_\ell$, the corresponding eigenenergies are

$$E_\ell=\frac{[\hbar\kappa_\ell]^2}{2M}=k_L^{-2}\left[\left(\frac{\pi\ell}{L}\right)^2-2\imath\sigma_\ell k_\ell\right]E_R. \quad (5)$$

A full set of quasibound states of center-of-mass motion of the (ground electronic state) atoms in the CAB cavity is therefore given by

$$\psi_{\ell uv}(\mathbf{r},t)=\chi_{uv}(x,y)\phi_\ell(z)\exp[-\imath(E_j+E_{uv})t/\hbar]. \quad (6)$$

We assume in the following that the potential barrier provided by the atomic mirrors is lower than the energy of the first excited transverse level, so that all trapped atoms are in the ground state $u=v=0$ of transverse motion.

In contrast to those ''atom laser'' schemes that rely solely on Bose enhancement to coherently populate one of the trap levels [1–3], our system uses explicitly two-body collisions to achieve laser action. For the situation at hand, the dominant source of atom-atom interactions is expected to be the near-resonant dipole-dipole interaction, whereby a photon spontaneously emitted by one atom is reabsorbed by a neighboring one. This long-range interaction is expected to dominate all other collisions at the densities we are interested in. Since it is important to reduce spontaneous heating as much as possible, the detuning Δ between the laser and atomic transition frequencies must be kept quite large, in which case the upper electronic levels can be adiabatically eliminated. In this regime, the atoms experience the two-dimensional transverse trapping potential [9]:

$$V(\mathbf{r})=\frac{\hbar|\Omega^{(+)}(\mathbf{r})|^2}{4(\Delta+\imath\gamma/2)}, \quad (7)$$

where $\Omega^{(\pm)}=2\boldsymbol{\mu}\cdot\mathbf{E}^{\pm}/\hbar$ are the Rabi frequencies of the two counterpropagating laser beams forming the transverse optical lattice,

$$\mathbf{E}^{\pm}=\mathscr{E}_0[\hat{\mathbf{e}}_x\cos k_Ly\pm\imath\hat{\mathbf{e}}_y\cos k_Lx]. \quad (8)$$

$\boldsymbol{\mu}$ is the dipole moment of the transition, and γ is its natural linewidth. In addition, ground-state atoms at the center-of-mass locations $\mathbf{r}$ and $\mathbf{r}'$ are subject to an effective two-body dipole-dipole potential whose explicit form in the case of two-level transitions is [9,11]

$$V_{dd}(\mathbf{r},\mathbf{r}')=\frac{\imath\hbar}{4(\Delta^2+\gamma^2/4)}\left[L(\mathbf{r}-\mathbf{r}')\Omega^{(+)}(\mathbf{r})\Omega^{(-)}(\mathbf{r}')+\frac{\gamma/2+\imath\Delta}{\gamma/2-\imath\Delta}L(\mathbf{r}-\mathbf{r}')^*\Omega^{(-)}(\mathbf{r})\Omega^{(+)}(\mathbf{r}')-\frac{|L(\mathbf{r}-\mathbf{r}')|^2}{\gamma/2-\imath\Delta}|\Omega^{(+)}(\mathbf{r}')|^2\right], \quad (9)$$

where

$$L(\mathbf{r}-\mathbf{r}')=\sum_{\mathbf{k}\lambda}\left[\frac{2\pi\omega_k}{\hbar V_e}\right]|\boldsymbol{\mu}\cdot\hat{\mathbf{e}}_{\mathbf{k}\lambda}|^2\left\{\left[\pi\delta(\omega_k-\omega_L)+P\left(\frac{\imath}{\omega_k-\omega_L}\right)\right]e^{-\imath\mathbf{k}\cdot(\mathbf{r}-\mathbf{r}')}+P\left(\frac{\imath}{\omega_k+\omega_L}\right)e^{\imath\mathbf{k}\cdot(\mathbf{r}-\mathbf{r}')}\right\}. \quad (10)$$

Here, the index λ labels the two orthogonal field modes corresponding to each wave vector $\mathbf{k}$, with polarization vectors

$\hat{\mathbf{e}}_{\mathbf{k}\lambda}$. In addition to the dipole-dipole potential V_{dd}, the dipole-dipole interaction also leads to additional contributions to atomic damping and fluctuations that are ignored here. Expanding the many-particle Schrödinger field operator onto the eigenstates basis of the resonator as

$$\Psi(\mathbf{r})=\sum_{\ell uv}\psi_{\ell uv}(\mathbf{r})c_{\ell uv}, \tag{11}$$

where the annihilation and creation operators $c_{\ell uv}$ and $c^{\dagger}_{\ell' u' v'}$ satisfy the boson commutation relations

$$[c_{\ell uv},c^{\dagger}_{\ell' u' v'}]=\delta_{\ell\ell'}\delta_{uu'}\delta_{vv'} \tag{12}$$

finally permits one to reexpress the second-quantized version of the dipole-dipole interaction V_{dd} as

$$\hat{V}_{dd}=\int d\mathbf{r}\int d\mathbf{r}'\Psi^{\dagger}(\mathbf{r})\Psi^{\dagger}(\mathbf{r}')V_{dd}(\mathbf{r},\mathbf{r}')\Psi(\mathbf{r}')\Psi(\mathbf{r})=\sum_{jlmn}\int d\mathbf{r}\int d\mathbf{r}'\psi_j^{*}(\mathbf{r})\psi_l^{*}(\mathbf{r}')V_{dd}(\mathbf{r},\mathbf{r}')\psi_m(\mathbf{r}')\psi_n(\mathbf{r})c_j^{\dagger}c_l^{\dagger}c_m c_n$$

$$\equiv\sum_{jlmn}V_{jlmn}, \tag{13}$$

where the indices are now composite indices including all three quantum numbers required to describe the center-of-mass state of the atoms. Since we consider only the ground electronic state of the atoms, and only the ground state of transverse motion, these labels actually label the longitudinal mode of motion.

III. SELECTION RULES

The selection rules obeyed by the dipole-dipole interaction are obtained by computing the matrix elements V_{jlmn} of the dipole-dipole potential for the explicit form (8) of the laser fields used to achieve the transverse confinement of the atoms. Integrating over $\mathbf{r}$ and $\mathbf{r}'$, going to the continuum limit $(1/V_e)\Sigma_{\mathbf{k}}\rightarrow(2\pi)^{-3}\int d^3k$, where V_e is the quantization volume, and integrating over $k=|\mathbf{k}|$ and over the azimuthal angle ϕ in reciprocal space yields then in the absence of losses

$$V_{jlmn}=\frac{8}{3}s_0\hbar\Gamma\left(\frac{k_L}{L}\right)^2 e^{-k_L^2W_T^2/2}k_jk_lk_mk_nc_j^{\dagger}c_l^{\dagger}c_mc_n\int_0^{\pi/2}\sin\theta\cos^2\theta d\theta e^{-k_L^2W_T^2\sin^2\theta/2}[I_0(k_L^2W_T^2\sin\theta)+1]$$

$$\times\frac{\mathcal{G}_{jlmn}(\theta)}{[k_L^2\cos^2\theta-(\kappa_j^{*}+\kappa_n)^2][k_L^2\cos^2\theta-(\kappa_j^{*}-\kappa_n)^2]}\times\frac{1}{[k_L^2\cos^2\theta-(\kappa_l^{*}+\kappa_m)^2][k_L^2\cos^2\theta-(\kappa_l^{*}-\kappa_m)^2]}, \tag{14}$$

where θ is the angle between $\mathbf{k}$ and the z axis, I_0 is a modified Bessel function of zeroth order, s_0 is the saturation parameter

$$s_0=\frac{\Omega_0^2/2}{\Delta^2+\gamma^2/4}, \tag{15}$$

where $\Omega_0=2\mathcal{E}_0|\mu|/\hbar$ is the Rabi frequency, and

$$\mathcal{G}_{jlmn}(\theta)=\begin{cases}0 & \text{if } j+n \text{ and } l+m \text{ have different parity}\\ 2[.\mathcal{S}(\sin\theta)+(-1)^{(j+n)}\sin(k_LL\cos\theta)] & \text{if } j+n \text{ and } l+m \text{ have the same parity}\end{cases} \tag{16}$$

establishes selection rules between the various modes of the resonator for the dipole-dipole interaction. The explicit form of $\mathcal{S}(\sin\theta)$ is

$$\mathcal{S}(\sin\theta)=\sqrt{\frac{2}{\pi}}e^{k_L^2W_T^2\sin^2\theta/2}\int_0^{\infty}dx e^{-x^2/2}\sin(k_LW_Tx\sin\theta). \tag{17}$$

The expressions (14) and (17) are still valid in the presence of small losses $\sigma_{\ell}\ll k_{\ell}$, and were obtained after disregarding terms describing self-energy contributions to the dipole-dipole interaction.

In order to analyze the impact of the resonance denominators in Eq. (14), we introduce the parameter s through $k_L\cos\theta=s\pi/L$. (Note that this parameter is normally noninteger.) The leading term in the numerator of Eq. (14) has a bell-shaped form as a function of θ in the interval $0\leqslant\theta\leqslant\pi/2$, and its maximum lies around $\theta_{\max}\approx\pi/4$ for $W_T\leqslant\lambda/4$. As W_T is increased the maximum moves towards higher values of θ. This indicates that for transversally well-confined atoms ($W_T\leqslant\lambda/4$), the dominant processes are those for which $\cos\theta=\cos\theta_{\max}\approx\sqrt{2}/2$. Equation (5) shows that in that case, and for negligible losses, the value $s=2L\cos\theta_{\max}/\lambda$ labels the longitudinal resonator mode of energy equal to half the recoil energy of the atoms. Restrict-

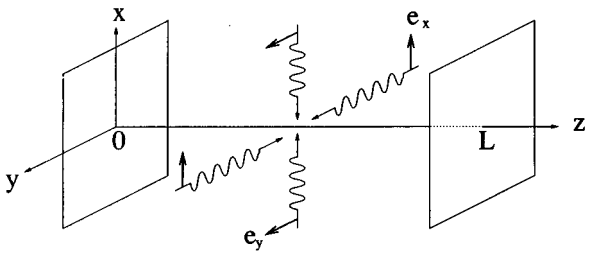

FIG. 1. Coherent atomic-beam generator cavity, illustrating the longitudinal confinement achieved by two mirrors for atoms at positions $z=0$ and $z=L$, as well as the transverse confinement achieved by two pairs of counterpropagating lasers in lin$\|$lin configurations.

ing our discussion to cavity modes with quantum numbers larger than s, we conclude then by inspection of the denominators in Eq. (14) that there are only two kinds of resonantly enhanced processes, corresponding to either $j-n=\pm s$ or $l-m=\pm s$. In physical terms, this indicates that the dominant matrix elements of the dipole interaction correspond to resonantly enhanced processes satisfying the ''momentum conservation'' condition

$$k_j-k_n=\pm(k_l-k_m)\approx k_L\cos\theta_{\max}. \tag{18}$$

The combinations of creation and annihilation operators associated with these elementary processes, as well as the corresponding changes in atomic center-of-mass energy, are summarized in Table I.

The resonance condition (18) indicates that the energy levels of the atomic resonator are predominantly coupled within manifolds separated in momentum by the wave number $(\sqrt{2}/2)k_L$, the coupling between manifolds being very weak. This suggests a simple approach to the theory of a ''laser for atoms,'' where only one manifold is considered in a first step. The contributions of the various manifolds can subsequently be incoherently added if necessary, in a manner reminiscent of inhomogeneously broadened laser theory. It should be noticed that good transverse confinement is essential to this approach, since the momentum spacing between levels within a manifold becomes smaller for weaker confinement.

TABLE I. Selection rules for the predominant dipole-dipole collisions.

		$n,m>s$	$\Delta E/E_R(\lambda/2L)^2$
$j-n=s$	$l-m=s$	$c^\dagger_{n+s}c^\dagger_{m+s}c_mc_n$	$2s^2+2s(m+n)$
	$l-m=-s$	$c^\dagger_{n+s}c^\dagger_{m-s}c_mc_n$	$2s^2-2s(m-n)$
$j-n=-s$	$l-m=s$	$c^\dagger_{n-s}c^\dagger_{m+s}c_mc_n$	$2s^2+2s(m-n)$
	$l-m=-s$	$c^\dagger_{n-s}c^\dagger_{m-s}c_mc_n$	$2s^2-2s(m+n)$

The number of bound states to be considered in a particular manifold depends of course on the height of the Fabry-Pérot potential barrier. Selective pumping into an excited cavity mode belonging to a specific manifold could, for instance, be achieved by resonant tunneling from a first stage resonator fed from a cold atomic cloud via Sisyphus cooling [12,16]. The output coupling could result, e.g., from turning off the optical mirrors, a rather crude but effective type of Q switching.

We can estimate the value of V_{jlmn} by setting $\cos^2\theta\approx\cos^2\theta_{\max}$ in the denominator of Eq. (14). With Eq. (18), and neglecting terms quadratic in the loss rates $\gamma_i=\hbar\sigma_ik_i/M$, yields

$$V_{jlmn}\approx -\imath\frac{\hbar s_0\Gamma}{3L^2}e^{-k_L^2W_T^2/2}\frac{c_j^\dagger c_l^\dagger c_mc_n}{[(\hbar\gamma_j/E_j)k_j+(\hbar\gamma_n/E_n)k_n][(\hbar\gamma_l/E_l)k_l+(\hbar\gamma_m/E_m)k_m]}||\mathscr{T}_{jlmn}||, \tag{19}$$

where the reduced dipole-dipole interaction matrix element $||\mathscr{T}_{jlmn}||$ is given by

$$||\mathscr{T}_{jlmn}||=\int_0^{\pi/2}\sin\theta d\theta e^{-k_L^2W_T^2\sin^2\theta/2}\cos^2\theta[I_0(k_L^2W_T^2\sin\theta)+1]\mathscr{G}_{jlmn}(\theta). \tag{20}$$

Terms of the form $\hbar\gamma_\ell$ in Eq. (19) represent the energy width of the Fabry-Pérot level ℓ. We see, then, that the strength of the dipole-dipole interaction depends on the specific cavity design through (i) the finite width of the Fabry-Pérot levels arising from tunneling losses, which can be estimated by assuming a rectangular optical potential barrier [17]; (ii) the intensity and detuning of the laser beams used for the transverse confinement of the atoms which determine the saturation parameter s_0; and finally (iii) the ratio of the longitudinal to transverse dimensions of the cavity.

IV. MASTER EQUATION

Using as a guide the discussion of the preceeding sections, we consider a model of a CAB including two levels of center-of-mass motion coupled to two separate reservoirs. The ''pump'' level $|3\rangle$ is taken to be the highest bound level of the resonator. It is pumped by a process sufficiently state selective that pumping into other levels can be neglected. For example, one possibility might involve a geometry consisting of two coupled cavities separated by a potential wall

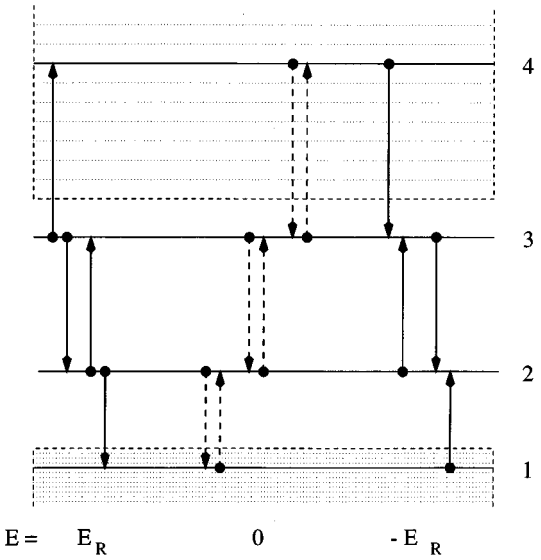

FIG. 2. Four-level scheme for a CBA generator. Level $|2\rangle$ is the ''lasing'' level, level $|3\rangle$ is the pump level, and levels $|1\rangle$ and $|4\rangle$ are treated as parts of two Markovian reservoirs, as discussed in the text. The collision processes with smallest energy defects are indicated by arrows. Dashed arrows represent collision processes that do not contribute to variations in level population. The energy defect related to each family of processes is specified at the bottom of the figure.

slightly lower than the external atomic mirrors. Pumping would then result from the escape of atoms from the initially filled ''pump'' cavity over this wall and into the initially empty ''laser'' cavity. (In that case, the level $|3\rangle$ would strictly speaking be shared by both cavities, but the two cavities could be considered as independent as far as their lower levels are concerned, provided that intercavity tunneling can be ignored.) Another possibility would involve quantum tunneling through the laser cavity mirrors, but the achievement of a significant pump rate would imply a broadening of the pump level that might not be acceptable.

As discussed earlier, the selectively pumped level $|3\rangle$ is predominantly coupled by the dipole-dipole interaction to a manifold of levels separated in momentum by integers of $(\sqrt{2}/2)k_L$. From all collision processes satisfying the momentum resonance condition (18), those associated with the smallest energy defect dominate the dynamics, as sketched in Fig. 2. Since elastic collisions do not change the populations of the various levels involved and hence yield only frequency shifts, the smallest relevant energy defects are $\Delta E=\pm E_R$. Collisions with $\Delta E=+E_R$ correspond to (a) the annihilation of two atoms from state $|3\rangle$, the creation of an atom in the continuum state $|4\rangle$, and the creation of one atom in the resonator bound state $|2\rangle$: or (b) the annihilation of two atoms from state $|2\rangle$ and the creation of atoms in states $|3\rangle$ and $|1\rangle$. The energy defect $-E_R$ corresponds to the reverse processes.

Since the levels in the manifold with energy higher than that of level $|2\rangle$ are by construction continuum levels, they are characterized by a free space density of states, and hence we proceed by treating level $|4\rangle$ as part of a thermal reservoir. Physically, this indicates that we make the quite reasonable assumption that once an atom has been excited to the continuum, it irreversibly escapes from the system. Level $|1\rangle$ is also treated as being part of a reservoir, this approximation resulting in this case from the observation that the density of bound states of the resonator increases as we move down the manifold in energy, a consequence of the quadratic dependence of energy on center-of-mass momentum. For example, for a cavity length of about 20 optical wavelengths, the energy separation between bound levels near the bottom of the potential well is about $2\times10^{-3}E_R$. This is much smaller than the energy defect E_R, so that near the bottom of atomic Fabry-Pérot, the center-of-mass energy levels can indeed be approximated as a continuum. These approximations lead to a simple ''two-level CAB'' model, where a pump level $|3\rangle$ and a ''lasing'' level $|2\rangle$ are coupled to each other as well as to two reservoirs symbolically labeled $|1\rangle$ and $|4\rangle$ via near-resonant dipole-dipole collisions. In addition, the pump level $|3\rangle$ is selectively pumped, e.g., by tunneling, and linear losses from the levels $|2\rangle$ and $|3\rangle$ are also included.

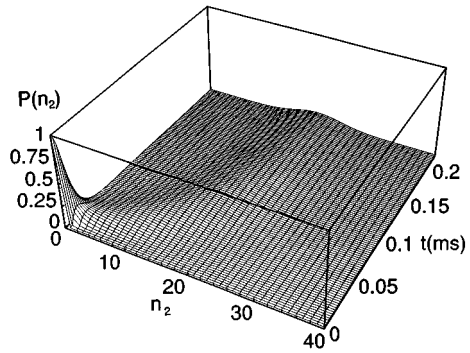

FIG. 3. Probability $P(n_2)$ of having n_2 atoms in level $|2\rangle$ as a function of n_2 and time. This plot is for $\alpha_1=0.2$, $\alpha_4=7.5$, $\beta_2=0.5$, $\beta_3=0.5$, and $\Lambda_3=600\ \mathrm{ms}^{-1}$, all rates being in units of ms^{-1}.

Adiabatically eliminating the reservoirs $|1\rangle$ and $|4\rangle$ in the Born-Markov approximation readily leads then to the CAB master equation

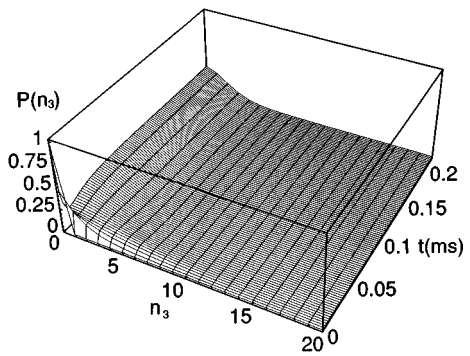

FIG. 4. Probability $P(n_3)$ of having n_3 atoms in level $|3\rangle$ as a function of n_3 and time. All parameters as in Fig. 3.

$$\frac{d\rho}{dt}=-\frac{\imath}{\hbar}[\hat{V}_{dd12},\rho]+\frac{\alpha_1}{2}(2c_3^\dagger c_2 c_2\rho c_2^\dagger c_3^\dagger-c_2^\dagger c_3^\dagger c_3 c_2 c_2\rho-\rho c_2^\dagger c_3^\dagger c_3 c_2 c_2)$$
$$+\frac{\alpha_4}{2}(2c_2^\dagger c_3 c_3\rho c_3^\dagger c_2^\dagger-c_3^\dagger c_2 c_2^\dagger c_3 c_3\rho-\rho c_3^\dagger c_2 c_2^\dagger c_3 c_3)+\frac{\beta_2}{2}(2c_2\rho c_2^\dagger-c_2^\dagger c_2\rho-\rho c_2^\dagger c_2)$$
$$+\left[\frac{\Lambda_3}{2}+\frac{\beta_3}{2}\right](2c_3\rho c_3^\dagger-c_3^\dagger c_3\rho-\rho c_3^\dagger c_3)+\frac{\Lambda_3}{2}(2c_3^\dagger\rho c_3-c_3 c_3^\dagger\rho-\rho c_3 c_3^\dagger), \tag{21}$$

which describes the dynamics of the two-level CAB. The first term on the right-hand side of this equation, proportional to $\hat{V}_{dd12}=V_{1212}c_1^\dagger c_2^\dagger c_1 c_2+V_{2323}c_2^\dagger c_3^\dagger c_2 c_3+\text{H.c.}$ does not contribute to the population dynamics of the CAB, as already discussed, but can give rise to energy shifts. The next two terms describe the coupling to the reservoirs, whose strength is given by $\alpha_1=2\pi\mathscr{D}(E_1/\hbar)|V_{2213}|^2/\hbar^2$ and $\alpha_4=2\pi\mathscr{D}(E_4/\hbar)|V_{2433}|^2/\hbar^2$ with $\mathscr{D}(E/\hbar)$ being the reservoir density of states at the energy E. Linear loss and pump rates have been phenomenologically added in their standard Lindblad form, with $\beta_i, i=2,3$ being linear loss rates and Λ_3 being the constant pump rate of level $|3\rangle$ [18].

From the master equation (21), we can readily derive equations of motion for the diagonal density matrix elements corresponding to the probabilities P_{n_2,n_3} of having n_2 and n_3 atoms in levels $|2\rangle$ and $|3\rangle$, respectively. These coupled equations have the form

$$\frac{dP_{n_2,n_3}}{dt}=\alpha_1[n_3(n_2+1)(n_2+2)P_{n_2+2,n_3-1}-n_2(n_2-1)(n_3+1)P_{n_2,n_3}]+\alpha_4[n_2(n_3+1)(n_3+2)P_{n_2-1,n_3+2}$$
$$-n_3(n_3-1)(n_2+1)P_{n_2,n_3}]+\beta_2[(n_2+1)P_{n_2+1,n_3}-n_2P_{n_2,n_3}]+\Lambda_3[n_3P_{n_2,n_3-1}-(n_3+1)P_{n_2,n_3}]+(\Lambda_3+\beta_3)$$
$$\times[(n_3+1)P_{n_2,n_3+1}-n_3P_{n_2,n_3}]. \tag{22}$$

V. DYNAMICS

In order to gain insight into the dynamics of the CAB, we have numerically solved the system of equations (22), assuming that at the initial time $t=0$ the cavity is empty and level $|3\rangle$ starts being pumped at the constant rate $\Lambda_3=600\ \text{ms}^{-1}$. The numerical values of the dipole-dipole rates α_1 and α_4, as well as those of the linear losses, can be substantially varied by modifying the cavity design, and we have chosen values close to those believed to be experimentally achievable. In our numerical work, we have varied the value of α_4 while keeping all other parameters constant.

Figure 3 shows an example of temporal evolution of the system where the population of the "lasing" level $|2\rangle$ builds up to a steady state with atom statistics $P(n_2)=\Sigma_{n_3}P_{n_2,n_3}$ reminiscent of the Poissonian photon statistics characteristic of a single mode laser. At $t=0$ the level is empty, and the probability of having 0 atoms is 1. But when the pump Λ_3 is turned on, the maximum of the probability distribution $P(n_2)$ is shifted towards $n_2\approx 30$ and a steady state is reached where the $P(n_2)$ is approximately Poissonian. A qualitatively different behavior is observed for the temporal evolution of the probability $P(n_3)=\Sigma_{n_2}P_{n_2,n_3}$ of having n_3 atoms in level $|3\rangle$, as shown in Fig. 4. This distribution becomes wider with time, but its maximum remains at $n_3=0$. In this regime, the mean population in level $|3\rangle$ remains low, and smaller than the mean population in level $|2\rangle$.

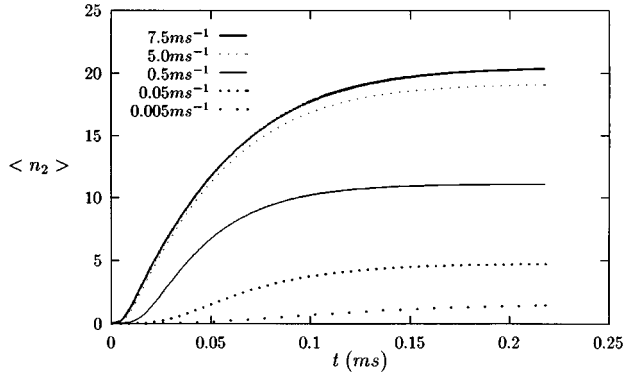

FIG. 5. Mean atomic population $\langle n_2\rangle$ in the "lasing level" as a function of time for various values of α_4, as indicated in the figure. All other parameters as in Fig. 3.

The behavior of the system as a function of α_4 is summarized in Figs. 5–8. The time evolution of the mean atomic population $\langle n_2\rangle$ of the "lasing" level is shown in Fig. 5. It increases with time and eventually reaches a steady-state value, which becomes larger with larger α_4. Figure 6 shows the normalized variance, or Fano factor

$$v_2=\frac{\langle n_2^2\rangle-\langle n_2\rangle^2}{\langle n_2\rangle} \tag{23}$$

of the "lasing" mode $|2\rangle$ as a function of time and for various values of α_4. (Figure 2 corresponds to the thick solid line on this figure.) Large fluctuations occur for short times, after which the system settles to a steady state. We observe that for large enough α_4, v_2 converges to a value approximately equal to 1, which corresponds to a Poissonian distribution. For smaller values of α_4, in contrast, the final atom statistics in mode $|2\rangle$ is always super-Poissonian. Note also

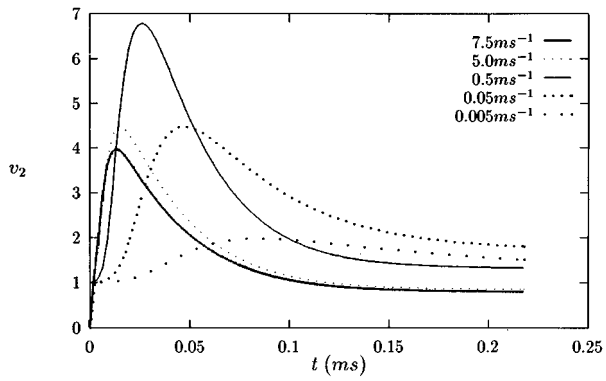

FIG. 6. Temporal dependence of the normalized variance v_2, or Fano factor, of the atom statistics in state $|2\rangle$. The various curves correspond to the values of α_4 specified in the figure. All other parameters as in Fig. 3.

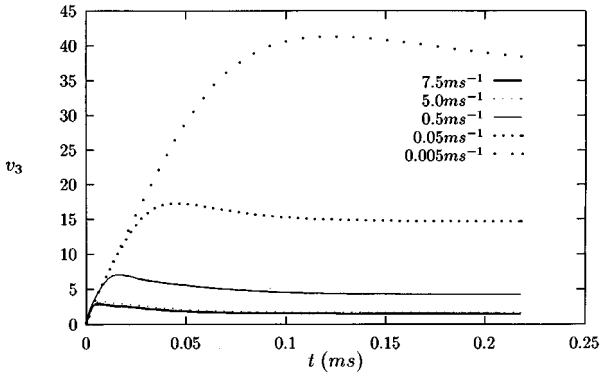

FIG. 8. Temporal dependence of the normalized variance v_3 of the atom statistics in state $|3\rangle$. The various curves correspond to the values of α_4 specified in the figure. All other parameters as in Fig. 3.

the large transient fluctuations for α_4 at the ''threshold'' between super-Poissonian and Poissonian steady-state atom statistics.

For comparison, Fig. 7 shows the mean atomic population $\langle n_3\rangle$ in level $|3\rangle$. We see that for α_4 well below threshold, the mean population $\langle n_3\rangle$ is quite large; since the coupling to the reservoir $|4\rangle$ and to the lasing level $|2\rangle$ is weak, level $|3\rangle$ is not significantly depleted. Above threshold, in contrast, the population of level $|3\rangle$ remains very small. The normalized variance v_3 of this level is shown in Fig. 8. Even above ''threshold,'' where the atom distribution in level $|2\rangle$ becomes Poissonian, the value of v_3 remains around 2, a signature of incoherent, super-Poissonian atom statistics.

VI. CONCLUSIONS

It has been realized for some time that two-body interactions such as the near-resonant dipole-dipole interaction lead to the appearance of nonlinear effects in atom optics. In this paper, we have shown how this nonlinearity can be used in the design of a coherent atomic beam generator, or ''atom laser.'' The specific system we have considered involves the use of the near-resonant dipole-dipole interaction between atoms in atomic resonators selectively pumped, e.g., via quantum tunneling. We determined that for transversally well-confined atoms, dipole-dipole collisions are resonantly enhanced when the atom-atom interactions involve momentum changes equal to $(\sqrt{2}/2)k_L$, k_L being the photon momentum of the lasers used to excite their dipoles. Hence, as the atoms collide their center-of-mass state moves up or down the eigenenergies ladder of the resonators in steps involving hundreds of resonator levels. This leads to the considerable simplification that all cavity levels except a few can effectively be treated either ignored or handled as a quasicontinuum, and therefore to a model of a coherent atomic-beam generator consisting of a ''two-level'' system coupled to two reservoirs via the dipole-dipole interaction. The first of these reservoirs describes levels near the bottom of the Fabry-Pérot, while the other describes unbound levels. Numerically solving the resulting master equation for the CAB dynamics, we demonstrated that a steady state with Poissonian population of the ''lasing level'' can be achieved if the dipole-dipole coupling between the pump and laser levels is strong enough.

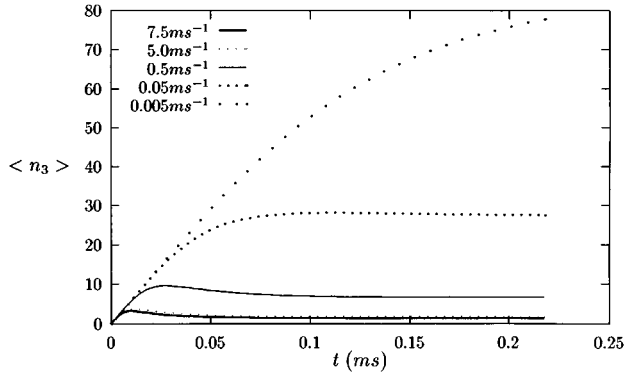

FIG. 7. Mean atomic population $\langle n_3\rangle$ of the pumping level $|3\rangle$ as a function of time for various values of α_4, as indicated in the figure. All other parameters as in Fig. 3.

There are still a number of open questions about the proposed coherent atomic-beam generator, and they will be addressed in subsequent work. For instance, we have so far concentrated only on the population of the various levels involved, but other correlation functions, involving nondiagonal elements of the atoms' density operator, promise to yield important information about the coherence of the generated beam. Also, we have used the idea of threshold very loosely here. Because the system under consideration has a very small size — the mean atom numbers in the ''lasing'' mode are only 30 or so, no sharp threshold is expected in this system. Yet, it will be interesting and useful to study the transition between incoherent and coherent output in more detail. Other aspects of our theory that require more attention include the analysis of pump mechanisms and the assumption that a number of cavity levels can be adequately treated as reservoirs. This ansatz will need to be tested against more detailed numerical work. Finally, we mentioned that the system we have investigated produces a rather weak mean population of the coherently populated cavity mode. It will be well worth investigating ways to improve the CAB output in the future.

ACKNOWLEDGMENTS

This work is funded by the U.S. Office of Naval Research Contract No. N00014-91-J1205, by the National Sciences Foundation Grant No. PHY95-07639, and by the Joint Services Optics Program. Part of this research was conducted using the resources of the Cornell Theory Center, which receives major funding from the National Science Foundation (NSF) and New York State, with additional support from the Advanced Research Projects Agency (ARPA), the National Center for Research Resources at the National Institutes of Health (NIH), IBM Corporation, and other members of the center's Corporate Research Institute. A.G. acknowledges financial support from COLCIENCIAS and Universidad Nacional de Colombia.

[1] H. M. Wiseman, M. J. Collett, Phys. Lett. A **202**, 246 (1995).
[2] R. J. C. Spreeuw, T. Pfau, U. Janicke, and M. Wilkens, Europhys. Lett. **32**, 469 (1995).
[3] M. Olshanii, Y. Castin, and J. Dalibard, in *Proceedings of the 12th International Conference on Laser Spectroscopy*, edited by M. Inguscio, M. Allegrini, and A. Lasso (World Scientific, Singapore, 1995).
[4] M. Holland, K. Burnett, C. Gardiner, J. I. Cirac, and P. Zoller (unpublished).
[5] M. H. Anderson, J. R. Ensher, M. R. Matthews, C. E. Wieman, and E. A. Cornell, Science **269**, 198 (1995).
[6] C. C. Bradley, C. A. Sackett, J. J. Tollett, and R. G. Hulet, Phys. Rev. Lett. **75**, 1687 (1995).
[7] W. Zhang, P. Meystre, and E. Wright, Phys. Rev. A **52**, 498 (1995).
[8] M. Wilkens, E. Goldstein, B. Taylor, and P. Meystre, Phys. Rev. A **47**, 2366 (1993).
[9] W. Zhang and D. F. Walls, Phys. Rev. A **49**, 3799 (1994).
[10] A. M. Smith and K. Burnett, J. Opt. Soc. Am. B **8**, 1592 (1991).
[11] G. Lenz and P. Meystre, Phys. Rev. A **48**, 3365 (1993).
[12] K. Berg-Sørensen, Y. Castin, E. Bonderup, and K. Mølmer, J. Phys. B **25**, 4195 (1992); K. Berg-Sørensen, Y. Castin, K. Mølmer, and J. Dalibard, Europhys. Lett. **22**, 663 (1993).
[13] P. S. Jessen, C. Gerz, P. D. Lett, W. D. Phillips, S. L. Rolston, R. J. C. Spreeuw, and C. I. Westbrook, Phys. Rev. Lett. **69**, 49 (1992).
[14] G. Grynberg, B. Lounis, P. Verkerk, J.-Y. Courtois, and C. Salomon, Phys. Rev. Lett. **70**, 2249 (1993).
[15] P. Verkerk, D. R. Meacher, A. B. Coates, J.-Y. Courtois, S. Guibal, B. Lounis, C. Salomon, and G. Grynberg, Europhys. Lett. **26**, 171 (1994).
[16] J. Dalibard and C. Cohen-Tannoudji, J. Opt. Soc. Am. B **6**, 2023 (1989).
[17] See, e.g., E. Merzbacher, *Quantum Mechanics* (Wiley, New York, 1961).
[18] P. Meystre and M. Sargent III, *Elements of Quantum Optics*, 2nd ed. (Springer-Verlag, Heidelberg, 1991).